DOI: 10.1002/adma.201103634

High magneto-optical activity and low optical losses in metal-dielectric Au/Co/Au – SiO_2 magnetoplasmonic nanodisks

By *Juan Carlos Banthí, David Meneses, Fernando García, María Ujué González, Antonio García-Martín, Alfonso Cebollada,** and *Gaspar Armelles*

[*] J.C. Banthí, Dr. D. Meneses, Dr. F. García, Dr. M.U. González, Dr. A. García-Martín, Prof. A. Cebollada, Prof. G. Armelles

IMM-Instituto de Microelectrónica de Madrid (CNM-CSIC), Isaac Newton 8, PTM, E-28760 Tres Cantos, Madrid, Spain
E-mail: alfonso@imm.cnm.csic.es

Keywords: ((Five maximum) magneto-optics, magnetoplasmonics, optical losses, nanodisks, plasmonics)

Combining materials with ferromagnetic and plasmonic properties has recently become an active area of research.[1-12] The generation of the so called magnetoplasmonic materials allows to study a wide variety of physical phenomena in which both characters (magnetic and plasmonic) are intertwined, i.e., it is possible to control one by acting on the other and vice versa.[13] For example, the plasmonic characteristics of different kinds of magnetoplasmonic structures can be tuned by the action of an external magnetic field, basically by its capability of acting on the off diagonal elements of the dielectric tensor of the system which, for the ferromagnetic material case, are sizable.[5,10,12,14,15] On the other hand, it is also possible to enhance the magneto-optical (MO) activity in continuous films and nanostructured magnetoplasmonic systems upon excitation of their characteristic surface plasmon resonances.[1,2,5-7,9,11,12,16,17] In this second case, since the MO activity is proportional to the electromagnetic (EM) field in the MO active material,[2,17-19] the physical mechanism lies on the light harvesting properties of the plasmonic system, which effectively concentrates the EM field in the MO active material region.

From an applied point of view, materials with increased MO activity are relevant in the context of telecommunications, where they could be used to construct ultra-fast optical

switches and integrated optical isolators/circulators elements; they also offer a potential for the development of high speed MO spatial light modulators for high density holographic data storage and 3D displays; and they could serve for magnetic field sensing as well.[20] Obtaining these materials is therefore pertinent for several application niches, and magnetoplasmonic systems constitute a very promising choice. Different kinds of magnetoplasmonic materials have been proposed so far, with the plasmonic material being a transition metal (Au, Ag, etc…) and the ferromagnetic component either a metal (Fe, Co, Ni)[5,6,9-11,13-16,21,22] or an oxide (Fe or Co oxides, or garnets).[7,12,23] In these magnetoplasmonic materials the enhancement of the MO activity comes along with an increase of the optical absorption, which limits their use in transmission related devices. The current situation still allows for further improvement, either by additional increasing of the MO activity, or by the reduction of the optical absorption.

In the present work we present our approach to reach this objective by performing a strong EM field redistribution at the nanoscale in metal-dielectric magnetoplasmonic materials, which takes place by inserting in adequate positions dielectric (SiO_2) layers into Au/Co/Au nanodisks. This dielectric layer insertion gives rise to hybrid plasmonic modes with a new distribution of the EM field.[24-26] We will show how by selecting the position of the dielectric layer inside the structure we have an effective way to increase the EM field in the MO active components (Co), while reducing it in the other non MO active, lossy elements, providing a system with enhanced MO activity and moderate absorption.

Three structures, Au/Co/SiO_2/Au, Au/SiO_2/Co/Au, and Au/Co/Au nanodisks, as sketched in **Figure 1a**, were fabricated by means of colloidal lithography and evaporation (see experimental section). The thickness of each layer is 15 nm for Au, 10 nm for Co and 20 nm for SiO_2. An identical amount of Au and Co was used in the Au/Co/Au structure in order to compare the modification induced in the MO response by the insertion of the SiO_2 layer. **Figure 1b** shows a representative AFM image of one of the fabricated systems. An ensemble

of nanodisks randomly distributed over the surface is clearly observable, with an average density around 7.5 x 10^8 disks /cm^2, and an average interdisk distance of 350 nm. This warrants the lack of electromagnetic interdisk interaction. The actual shape of the nanodisks is that of truncated cones,[25,26] and approximate values of the upper and lower nanodisk diameters are 70nm and 110nm respectively, with slightly larger values for the fully metallic nanodisks.

In **Figure 2a** we present the extinction spectrum at normal incidence for the Au/Co/SiO_2/Au nanodisk structure (solid line). The spectrum has a clear extinction peak around 750 nm, position which from now on we denote as HWP (High Wavelength Peak), and a shoulder around 600 nm (LWP, Low Wavelength Peak), which is consistent with the results obtained in Au/SiO_2/Au nanodisks, [24] with some small differences due to the presence of Co, which damps and blueshifts the resonances.[13] The presence of Co in the structure also makes it exhibit magneto-optical activity, whose spectral dependence in the same wavelength range is shown in Figure 2c. Here we depict as a continuous line the measured intensity of the magneto-optical activity I_Φ for this structure, defined as the modulus ($I_\Phi = \sqrt{\theta^2 + \varphi^2}$) of the complex Kerr rotation of the structure, Φ ($\Phi=\theta+i\varphi$), being θ the Kerr rotation and φ the Kerr ellipticity. As it can be observed, two features are present: one in the HWP region and another one in the LWP region. For comparison, the extinction spectrum and the MO activity for the Au/Co/Au nanodisks sample are also plotted in Figures 2a and 2c as dashed lines. As it can be observed, this sample has only one peak located between the two features of the Au/Co/SiO_2/Au nanodisk structure.[27] This is related to the localized surface plasmon resonance (LSPR) of the Au/Co/Au nanodisks, which induces an enhancement in the MO activity.[6] The effect of inserting a SiO_2 layer into the Au/Co/Au nanodisk is to split this resonance into two resonances, originating from the localized plasmons of the top (Au/Co) and bottom (Au) metallic nanodisks separated by the SiO_2 layer. In this structure, it can be appreciated a correspondence between optical extinction and MO activity: the higher the

extinction, the stronger the MO activity, which is consistent with previous studies in this kind of systems.[6,7,11]

On the other hand, if the SiO_2 layer is placed in between the top Au layer and the Co layer i.e., if the nanodisk structure is Au/SiO_2/Co/Au, a drastic change in the optical response is observed with respect to the previous case. As it can be seen in **Figure 3a**, now the spectrum appears reversed, exhibiting a peak at the LWP region with just a shoulder on the region of the HWP. The complex Kerr rotation spectrum (Figure 3c) is, however, very similar to the spectrum of the preceding sample, with a peak in the MO activity in the spectral region of the HWP and a shoulder in the LWP region. Remarkably, this implies that in this specific structure we obtain high MO activity for a configuration corresponding to low optical extinction in the HWP region, contradicting the naïve rule of thumb that a larger absorption provides a larger MO activity.

These results indicate that first, the insertion of the SiO_2 layer within the nanodisk structure induces strong modifications in their extinction properties, and second the specific position of this layer allows controlling the spectral region where the optical extinction is maximized or minimized. Regarding the MO activity for both nanodisks samples, it is larger than that of the fully metallic structure with equivalent amount of Au and Co in the nanodisks, and moreover a larger extinction does not necessarily implies a larger MO activity.

In order to get further insight of the physical mechanism underlying these effects, we have performed numerical simulations (see details in the experimental section). The results for the extinction and MO activity are depicted in Figures 2b, 2d, 3b and 3d, showing an excellent agreement with the experiments, therefore confirming the validity of the used modeling to describe our experimental structures. Since both optical absorption and MO activity are ruled by the magnitude of the EM field in the optically absorbing and MO active components of the systems respectively,[2,17-19] in **Figure 4** we also show the spatial distribution of the intensity of the EM field (namely the square of the modulus of the electric field) along the YZ plane for

both metal-dielectric structures at the LWP (left) and the HWP (right) spectral regions. (As a reference, the EM field distribution of similar Au/Co/Au nanodisks can be found in Ref. [17].) Regarding the Au/Co/SiO_2/Au nanodisk structure, we can see that the amount of EM field for both spectral regions is larger in the bottom Au disk. Additionally, comparing both spectral regions, the EM field is larger for the HWP region than for the LWP region. This explains the larger optical absorption obtained in the HWP region for this structure. On the other hand, for the Au/SiO_2/Co/Au nanodisk structure, the EM field for both LWP and HWP regions is larger near the top Au disk. Comparing both spectral regions, the EM field now is larger in the LWP region than in the HWP one. Again, the larger EM field concentration in the absorbing components of the structure in the LWP in this specific case allows understanding the larger optical extinction observed in this spectral region. On the other hand, the values of the total intensity of the EM field inside the Co layer (related with the MO activity) are very similar for the two structures and the two spectral regions, which explains the similar MO activity observed for the two samples.[28] These findings indicate that, while the EM field in the whole structure governs the extinction response of the system, the value in the Co layer is the main responsible of the MO activity and therefore both magnitudes can be decoupled providing us a way to design magnetoplasmonic systems with low absorption and high magneto-optical activity.

For transmission related applications, it is convenient to compare simultaneously the MO activity and optical extinction, by defining a relevant figure of merit, which can be the ratio between the MO activity and the optical extinction, MO/Ext. This magnitude takes into account on one hand the pure MO activity of the structure and on the other its optical losses. In **Figure 5** we present the spectral dependence of this ratio, obtained from the experimental data, for the two metal-dielectric structures, with the corresponding equivalent structure without the SiO_2 spacer. Regarding the Au/Co/SiO_2/Au structure, two clear peaks are observed around LWP and HWP. The HWP peak is due to the characteristic large MO

activity of the structure in this spectral region, while the LWP is due (in spite of the lower MO activity) to the low optical extinction at this wavelength. On the other hand, for the Au/SiO_2/Co/Au structure, mainly a single peak, more intense than those obtained for the other structure, is observed in the HWP region, which is due to the simultaneous large MO activity and low optical absorption characteristic for this wavelength. The influence of inserting a dielectric layer in this figure of merit can be more clearly seen if we compare it with that for the fully metallic structure, which exhibits lower values than those for the metal-dielectric structures, and a pretty featureless spectral behavior. In this case, the weak maximum in the HWP region is simply due to the low extinction values of the fully metallic system in this region, but with no relevant MO activity being present.

For a comparison of these metal-dielectric magnetoplasmonic nanodisks with other MO materials relevant in transmission related applications, we have calculated the modulus of Faraday rotation divided by the transmission. In the spectral range where the metal-dielectric structures have low extinction this ratio is of the same magnitude than the calculated for a Bi-substitute YFe_2O_5 garnet structure[29] and higher than the calculated one for materials made from Fe or Co oxide nanoparticles embedded in a dielectric matrix.[30,31] This opens the door to the use of magnetoplasmonic materials in such devices. Moreover, since the wavelength position of the resonances obtained in these metal-dielectric nanodisks can be controlled by simply modifying their structural parameters (diameter, layer thickness), it will be possible to tune the spectral position at which the optical absorption is reduced and the MO activity maximized.

In conclusion, simultaneous large MO activity and low optical losses are obtained in Au/Co/Au magnetoplasmonic nanodisks in which a SiO_2 dielectric layer is inserted at specific positions within the nanostructure. These effects are particularly important at wavelengths where characteristic resonant modes of the nanodisks are excited. The main effect of inserting

the dielectric layer in the nanodisks is a strong redistribution of the electromagnetic (EM) field inside the structure upon plasmon resonance excitation, increasing the EM field in the MO active layer (Co) with its simultaneous reduction in the other absorbing but non MO active components of the system. The polarization conversion versus optical extinction figure of merit of these novel systems could be spectrally tuned by an adequate selection of the internal parameters of the nanodisks.

Experimental

Nanodisks fabrication: The nanodisks samples were fabricated by means of colloidal lithography [32] and evaporation. The colloidal lithography procedure provides the hole-mask templates and is the following. First, polystyrene colloidal particles (8% w/v, 100 nm, sulfate latex, INVITROGEN) were deposited by electrostatic self-assembly onto glass substrate precoated with ~360 nm of poly(methyl methacrylate) (PMMA, 4 wt % diluted in anisole, MW 950000, Microchem Corp.). The surface of the PMMA was treated with an oxygen plasma (50W, 450 mTorr) to make it hydrophilic, and then a single layer precursor film was adsorbed to make the surface positively charged using 0.02% (by weight) poly(diallylmethylammonium chloride) (PDDA, MW 400 000-/500 000, Sigma Aldrich), rinsing in water during 60 s and finally drying with nitrogen gas. Negatively charged polystyrene particles are adsorbed onto the charged substrates from solution by electrostatic interactions. Particle concentrations of 0.02% (by weight) were used. Adsorption time was 1 min to allow the adsorption to reach saturation and a better uniform distribution in all experiments. Excess particles were rinsed off under running water and the samples were blown dry with nitrogen gas. Milli-Q water (Millipore) was used at all times. The density of spheres was selected to obtain a disk concentration of 12%. After this, Au thin films (15 nm) were deposited by thermal evaporation. Polystyrene particles were retired of the surface substrate using tape striping, and then the sample undergoes an oxygen plasma treatment (50

sccm O_2, 50 W, 20ºC, $1x10^{-5}$ Torr, 90s) which attacks the Au uncovered PMMA and drill the holes. Subsequently, the templates were introduced in a UHV deposition system where, after deposition of 2nm Ti to improve the adhesion of the disks to the substrates, the corresponding Au, Co, SiO_2 layers for each structure were grown. Ti, SiO_2 and Co were deposited by electron beam deposition (0.1 A/sec; 0.5 A/sec and 0.25 A/sec deposition rates respectively with a pressure between 10^{-8}-10^{-9} mbar during deposition) and Au by thermal evaporation (0.25 A/sec deposition rate). After acetone based lift-off, an ensemble of nanodisks randomly oriented on the glass substrate was obtained.

Optical characterization: Extinction spectra were acquired by means of a spectrometer (Andor, Shamrock SR-303i) coupled by optical fiber to an Olympus microscope in bright field transmission configuration. Illumination was performed through a condenser with 0.1 N.A. and the light was collected with a low numerical aperture objective (x2, N.A. 0.06). The area from which the optical signal is collected is a circle with 300 μm diameter.

Magneto-optical characterization: The MO characterization of the samples has been carried out by means of Kerr (reflection) spectroscopy in the polar configuration. The sample, placed inside an electromagnet that applies a magnetic field perpendicular to its surface, is illuminated at normal incidence by a monochromatic beam coming from a Xe lamp followed by a monochromator. By modulating the beam polarization with a photoelastic modulator and recovering the reflected intensity with a photomultiplier using a lock-in configuration, the Kerr rotation and ellipticity for each wavelength are determined [33]. The measurements have been performed with an applied magnetic field which insures magnetic saturation of the structures.

Numerical calculations: Numerical simulations have been performed using two complementary methodologies, one fully developed by the authors based on the scattering matrix method (SMM) and adapted to be able to consider magneto-optical elements [34], and the second one based on the finite difference time domain (FDTD) (proprietary software by

Lumerical Solutions). In both cases the calculations were made upon normal illumination by a plane wave linearly polarized along the x-direction, and the truncated cone shape of the nanodisks has been introduced by stacking cylinders of decreasing diameter (see sketch in Figure 4). In the SMM we used a base of 1521 k-points and in the FDTD a real space grid with more than 40 points per wavelength in each direction. In all cases the optical and MO constants employed have been taken from ellipsometric and polar Kerr measurements performed on thin films grown by the same technique as those used in the present experiments [21]. Periodic boundary conditions have been used in both cases, ensuring that the disk concentration is the same as that of the experiments. The use of periodic boundary conditions is adequate because the average interdisk distance (350nm) is large enough so that interaction between disks is not important and also small enough not to introduce diffraction effects.

Acknowledgements
The authors acknowledge funding support from the EU (NMP3-SL-2008-214107-Nanomagma), the Spanish MICINN ("FUNCOAT" CONSOLIDER INGENIO 2010 CSD2008-00023, MAGPLAS MAT2008-06765-C02-01/NAN and PLASMAR MAT2010-10123-E) and the Comunidad de Madrid ("NANOBIOMAGNET", S2009/MAT-1726 and "MICROSERES-CM", S2009/ TIC-1476, and JAE Doc fellowship for D. Meneses-Rodríguez).

References

[1] V. I. Safarov, V. A. Kosobukin, C. Hermann, G. Lampel, J. Peretti, C. Marlière, *Phys. Rev. Lett.* **1994**, *73*, 3584.

[2] C. Hermann, V. A. Kosobukin, G. Lampel, J. Peretti, V. I. Safarov, P. Bertrand, *Phys. Rev. B* **2001**, *64*, 235422.

[3] G. Düchs, G. L. J. A. Rikken, T. Grenet, P. Wyder, *Phys. Rev. Lett.* **2001**, *87*, 127402.

[4] K. J. Chau, M. Johnson, A. Y. Elezzabi, *Phys. Rev. Lett.* **2007**, *98*, 133901.

[5] J. B. González-Díaz, A. García-Martín, G. Armelles, J. M. García-Martín, C. Clavero, A. Cebollada, R. A. Lukaszew, J. R. Skuza, D. P. Kumah, R. Clarke, *Phys. Rev. B* **2007**, *76*, 153402.

[6] J. B. González-Díaz, A. García-Martín, J. M. García-Martín, A. Cebollada, G. Armelles, B. Sepúlveda, Y. Alaverdyan, M. Käll, *Small* **2008**, *4*, 202.

[7] P. K. Jain, Y. Xiao, R. Walsworth, A. E. Cohen, *Nano Lett.* **2009**, *9*, 1644.

[8] L. Bogani, L. Cavigli, C. de Julián Fernández, P. Mazzoldi, G. Mattei, M. Gurioli, M. Dressel, D. Gatteschi, *Adv. Mater.* **2010**, *22*, 4054.

[9] G. X. Du, T. Mori, M. Suzuki, S. Saito, H. Fukuda, M. Takahashi, *Appl. Phys. Lett.* **2010**, *96*, 081915.

[10] V. V. Temnov, G. Armelles, U. Woggon, D. Guzatov, A. Cebollada, A. Garcia-Martin, J. M. Garcia-Martin, T. Thomay, A. Leitenstorfer, R. Bratschitsch, *Nat. Photonics* **2010**, *4*, 107.

[11] L. Wang, C. Clavero, Z. Huba, K. J. Carroll, E. E. Carpenter, D. Gu, R. A. Lukaszew, *Nano Lett.* **2011**, *11*, 1237.

[12] V. I. Belotelov, I. A. Akimov, M. Pohl, V. A. Kotov, S. Kasture, A. S. Vengurlekar, A. V. Gopal, D. R. Yakovlev, A. K. Zvezdin, M. Bayer, *Nat. Nanotechnol.* **2011**, *6*, 370.

[13] G. Armelles, A. Cebollada, A. Garcia-Martin, J. M. Garcia-Martin, M. U. Gonzalez, J. B. Gonzalez-Diaz, E. Ferreiro-Vila, J. F. Torrado, *J. Opt. A: Pure Appl. Opt.* **2009**, *11*, 114023.

[14] D. Martín-Becerra, J. B. González-Díaz, V. V. Temnov, A. Cebollada, G. Armelles, T. Thomay, A. Leitenstorfer, R. Bratschitsch, A. García-Martín, M. U. González, *Appl. Phys. Lett.* **2010**, *97*, 183114.

[15] J. F. Torrado, J. B. González-Díaz, M. U. González, A. García-Martín, G. Armelles, *Opt. Express* **2010**, *18*, 15635.

[16] G. Armelles, J. B. González-Díaz, A. García-Martín, J. M. García-Martín, A. Cebollada, M. U. González, S. Acimovic, J. Cesario, R. Quidant, G. Badenes, *Opt. Express* **2008**, *16*, 16104.

[17] D. Meneses-Rodríguez, E. Ferreiro-Vila, P. Prieto, J. Anguita, M. U. González, J. M. García-Martín, A. Cebollada, A. García-Martín, G. Armelles, *Small* **2011**, *accepted for publication*, DOI: 10.1002/smll.201101060.

[18] P. Bertrand, C. Hermann, G. Lampel, J. Peretti, V. I. Safarov, *Phys. Rev. B* **2001**, *64*, 235421.

[19] C. Clavero, K. Yang, J. R. Skuza, R. A. Lukaszew, *Opt. Express* **2010**, *18*, 7743.

[20] M. Inoue, A. Khanikaev, A. Baryshev, in *Nanoscale Magnetic Materials and Applications* (Eds.: J.P. Liu, E. Fullerton, O. Gutfleisch, D.J. Sellmyer), Springer, Boston, MA, **2009**, pp. 627-659.

[21] E. Ferreiro-Vila, J. B. González-Díaz, R. Fermento, M. U. González, A. García-Martín, J. M. García-Martín, A. Cebollada, G. Armelles, D. Meneses-Rodríguez, E. Muñoz-Sandoval, *Phys. Rev. B* **2009**, *80*, 125132.

[22] K. Yang, C. Clavero, J. R. Skuza, M. Varela, R. A. Lukaszew, *J. Appl. Phys.* **2010**, *107*, 103924.

[23] H. Uchida, Y. Masuda, R. Fujikawa, A. V. Baryshev, M. Inoue, *J. Magn. Magn. Mater.* **2009**, *321*, 843.

[24] A. Dmitriev, T. Pakizeh, M. Käll, D. S. Sutherland, *Small* **2007**, *3*, 294.

[25] T. Pakizeh, A. Dmitriev, M. S. Abrishamian, N. Granpayeh, M. Käll, *J. Opt. Soc. Am. B* **2008**, *25*, 659.

[26] Y. Ekinci, A. Christ, M. Agio, O. J. F. Martin, H. H. Solak, J. F. Löffler, *Opt. Express* **2008**, *16*, 13287.

[27] Note that the slightly larger diameter of these metallic nanodiscs leads to a larger extinction due to their specific aspect ratio, and to the larger total amount of absorbent material compared to the metal-dielectric nanodisks with smaller diameters.

[28] For example, the ratio between the EM field intensity inside the Co layer of the two structures ($I_\Phi(Au/Co/SiO_2/Au)/I_\Phi(Au/SiO_2/Co/Au)$) is 0.9 for the LWP region and 0.6 for the HWP region (in agreement with the similar MO spectra observed for the two structures). The same ratio but for the intensity of the EM field inside the three metallic layers, on the other hand, is 5 and 0.2 for the LWP and HWP, respectively, which explains the differences observed in the absorption spectra of the two structures.

[29] V. Doormann, J.-P. Krumme, H. Lenz, *J. Appl. Phys.* **1990**, *68*, 3544.

[30] F. Royer, D. Jamon, J. J. Rousseau, H. Roux, D. Zins, V. Cabuil, *Appl. Phys. Lett.* **2005**, *86*, 011107.

[31] F. Choueikani, F. Royer, D. Jamon, A. Siblini, J. J. Rousseau, S. Neveu, J. Charara, *Appl. Phys. Lett.* **2009**, *94*, 051113.

[32] H. Fredriksson, Y. Alaverdyan, A. Dmitriev, C. Langhammer, D. S. Sutherland, M. Zäch, B. Kasemo, *Adv. Mater.* **2007**, *19*, 4297.

[33] W. S. Kim, M. Aderholz, W. Kleemann, *Meas. Sci. Technol.* **1993**, *4*, 1275.

[34] A. García-Martín, G. Armelles, S. Pereira, *Phys. Rev. B* **2005**, *71*, 205116.

Figure Captions:

Figure 1. a) Sketch of the composition of the fabricated nanodisks. b) AFM image of a selected fabricated structure (15nmAu/10nmCo/20nmSiO_2/15nmAu).

Figure 2. a) Experimental extinction spectrum for the metal-dielectric Au/Co/SiO_2/Au structure (15nmAu/10nmCo/20nmSiO_2/15nmAu): solid line. The experimental spectrum for the fully metallic Au/Co/Au structure (15nmAu/10nmCo/15nmAu) is also plotted for comparison: dashed line. c) Experimental MO activity spectra for the metal-dielectric structure (solid line) and the fully metallic structure (dashed line). Calculated extinction, b) and MO activity, d), spectra, based on a scattering matrix formalism, for the metal-dielectric structure (solid line) and the fully metallic structure (dashed line).

Figure 3. a) Experimental extinction spectrum for the metal-dielectric Au/SiO_2/Co/Au structure (15nmAu/20nmSiO_2/10nmCo/15nmAu): solid line. The experimental spectrum for the fully metallic Au/Co/Au structure (15nmAu/10nmCo/15nmAu) is also plotted for comparison: dashed line. c) Experimental MO activity spectra for the metal-dielectric structure (solid line) and the fully metallic structure (dashed line). Calculated extinction, b) and MO activity, d), spectra, based on a scattering matrix formalism, for the metal-dielectric structure (solid line) and the fully metallic structure (dashed line).

Figure 4. Calculated spatial distribution along YZ plane of the EM field (square of the modulus of the electric field, $|E|^2$), obtained through FDTD simulations, for: a) Au/Co/SiO_2/Au nanodisk at the LWP spectral region; b) Au/Co/SiO_2/Au nanodisk at the HWP spectral; c) Au/SiO_2/Co/Au nanodisk at the LWP spectral region; d) Au/SiO_2/Co/Au nanodisk at the HWP spectral region. The upper and lower sketches in the left side of the figure represent the modeling of the nanodisk structures, whose shape of truncated cones has

been taken into account by means of cylinders of decreasing diameter. The illumination conditions are also shown in the middle scheme. Notice here that incoming beam polarization is along XZ plane, while the EM field intensity is depicted along the YZ plane. The LSP resonances excited in the nanodisks are of dipolar character, which is evident for EM field plots along the XZ plane, but due to the strong enhancement outside the structures, all the interior EM field distribution (the relevant one in terms of amount of field in the Co layer) is smeared out.

Figure 5. Experimental ratio between the MO activity and the optical extinction, MO/Ext, for the two metal-dielectric (thick solid and dashed lines) and fully metallic (thin solid line) structures.

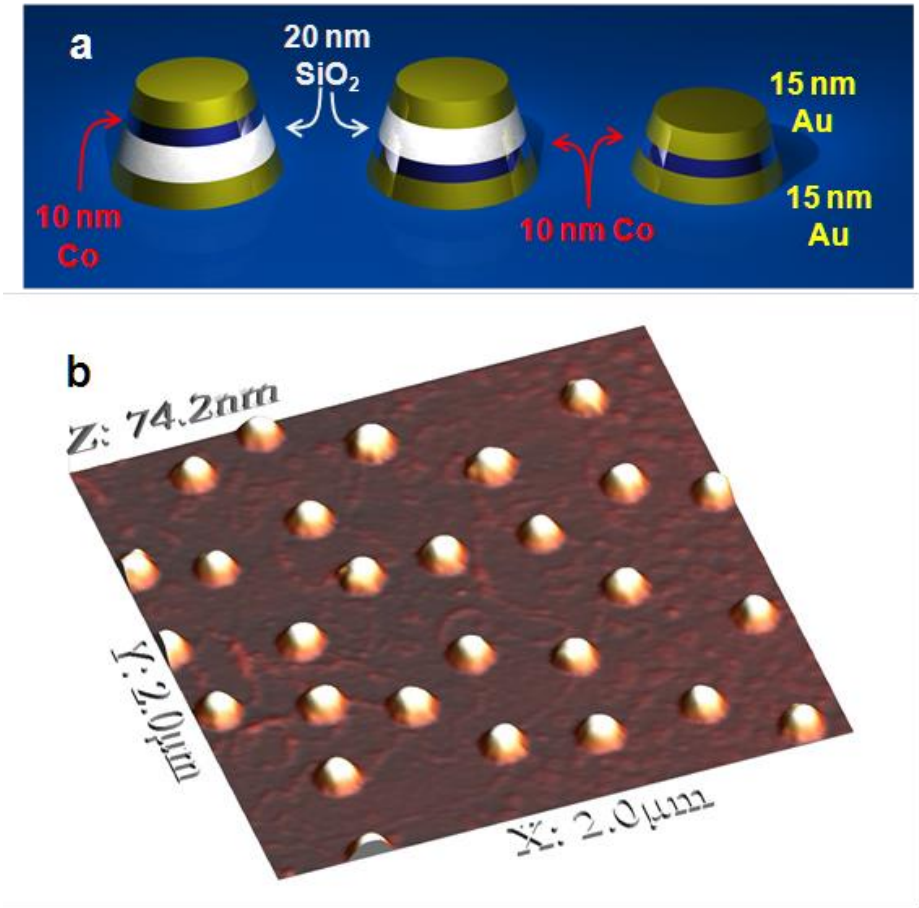

Figure 1. a) Sketch of the composition of the fabricated nanodisks. b) AFM image of a selected fabricated structure (15nmAu/10nmCo/20nmSiO_2/15nmAu).

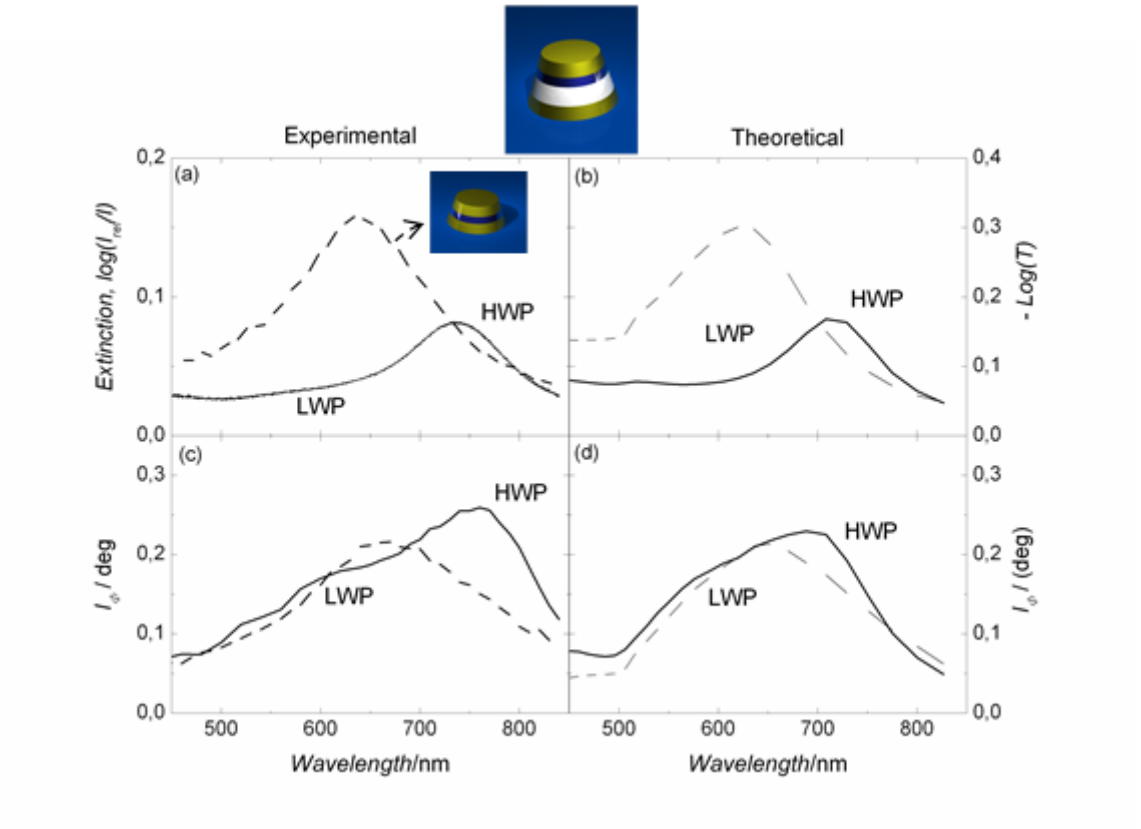

Figure 2. a) Experimental extinction spectrum for the metal-dielectric Au/Co/SiO_2/Au structure (15nmAu/10nmCo/20nmSiO_2/15nmAu): solid line. The experimental spectrum for the fully metallic Au/Co/Au structure (15nmAu/10nmCo/15nmAu) is also plotted for comparison: dashed line. c) Experimental MO activity spectra for the metal-dielectric structure (solid line) and the fully metallic structure (dashed line). Calculated extinction, b) and MO activity, d), spectra, based on a scattering matrix formalism, for the metal-dielectric structure (solid line) and the fully metallic structure (dashed line).

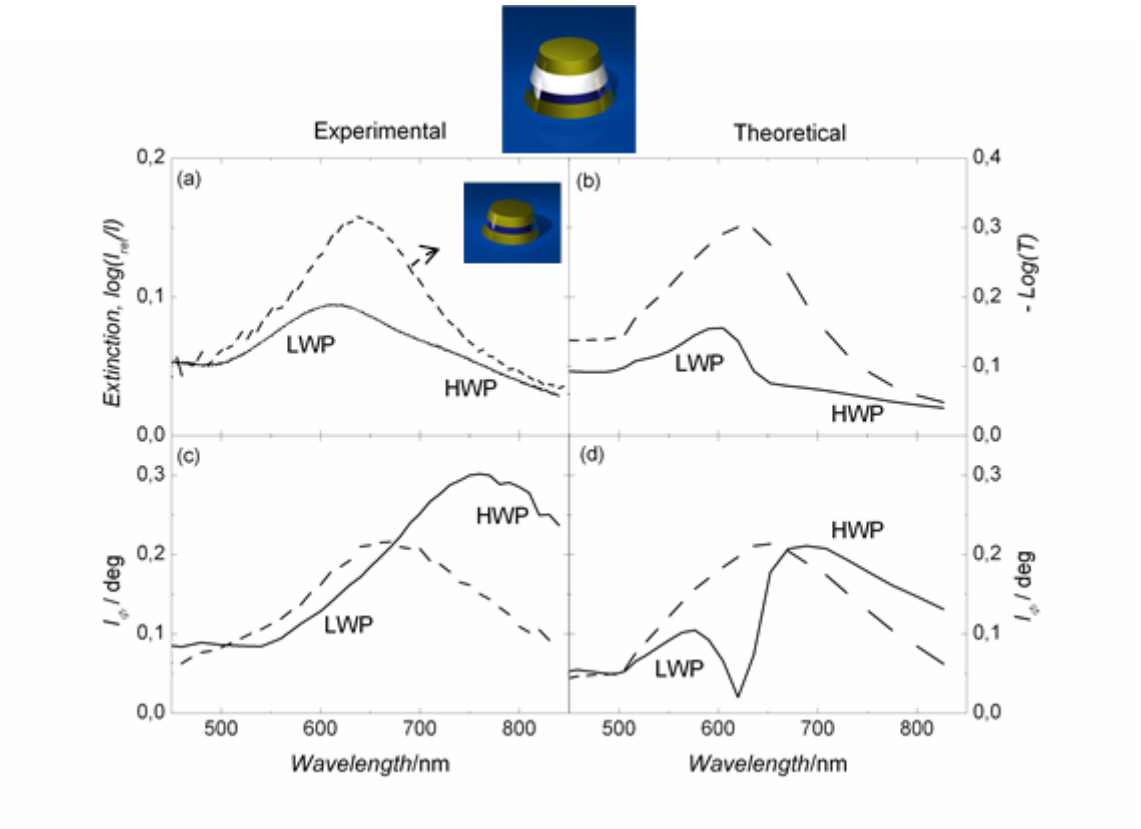

Figure 3. a) Experimental extinction spectrum for the metal-dielectric Au/SiO_2/Co/Au structure (15nmAu/20nmSiO_2/10nmCo/15nmAu): solid line. The experimental spectrum for the fully metallic Au/Co/Au structure (15nmAu/10nmCo/15nmAu) is also plotted for comparison: dashed line. c) Experimental MO activity spectra for the metal-dielectric structure (solid line) and the fully metallic structure (dashed line). Calculated extinction, b) and MO activity, d), spectra, based on a scattering matrix formalism, for the metal-dielectric structure (solid line) and the fully metallic structure (dashed line).

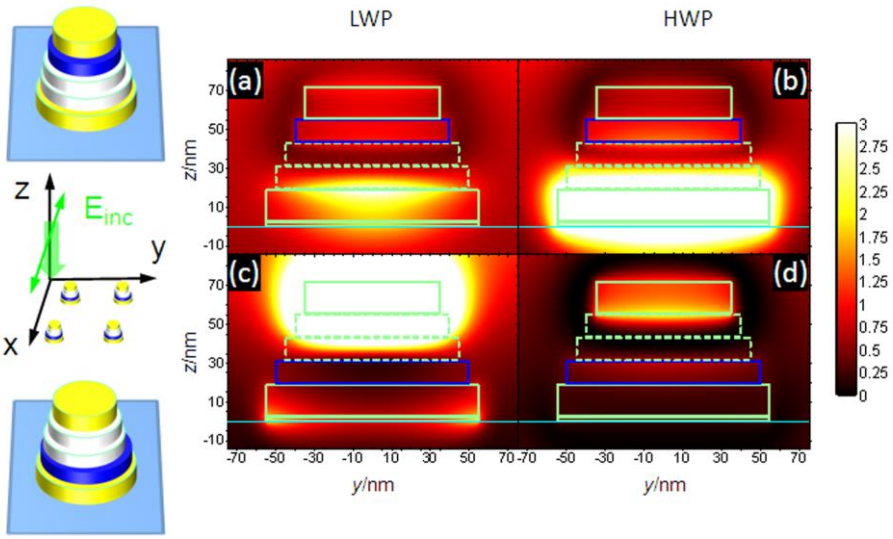

Figure 4. Calculated spatial distribution along YZ plane of the EM field (square of the modulus of the electric field, $|E|^2$), obtained through FDTD simulations, for: a) Au/Co/SiO_2/Au nanodisk at the LWP spectral region; b) Au/Co/SiO_2/Au nanodisk at the HWP spectral; c) Au/SiO_2/Co/Au nanodisk at the LWP spectral region; d) Au/SiO_2/Co/Au nanodisk at the HWP spectral region. The upper and lower sketches in the left side of the figure represent the modeling of the nanodisk structures, whose shape of truncated cones has been taken into account by means of cylinders of decreasing diameter. The illumination conditions are also shown in the middle scheme. Notice here that incoming beam polarization is along XZ plane, while the EM field intensity is depicted along the YZ plane. The LSP resonances excited in the nanodisks are of dipolar character, which is evident for EM field plots along the XZ plane, but due to the strong enhancement outside the structures, all the interior EM field distribution (the relevant one in terms of amount of field in the Co layer) is smeared out.

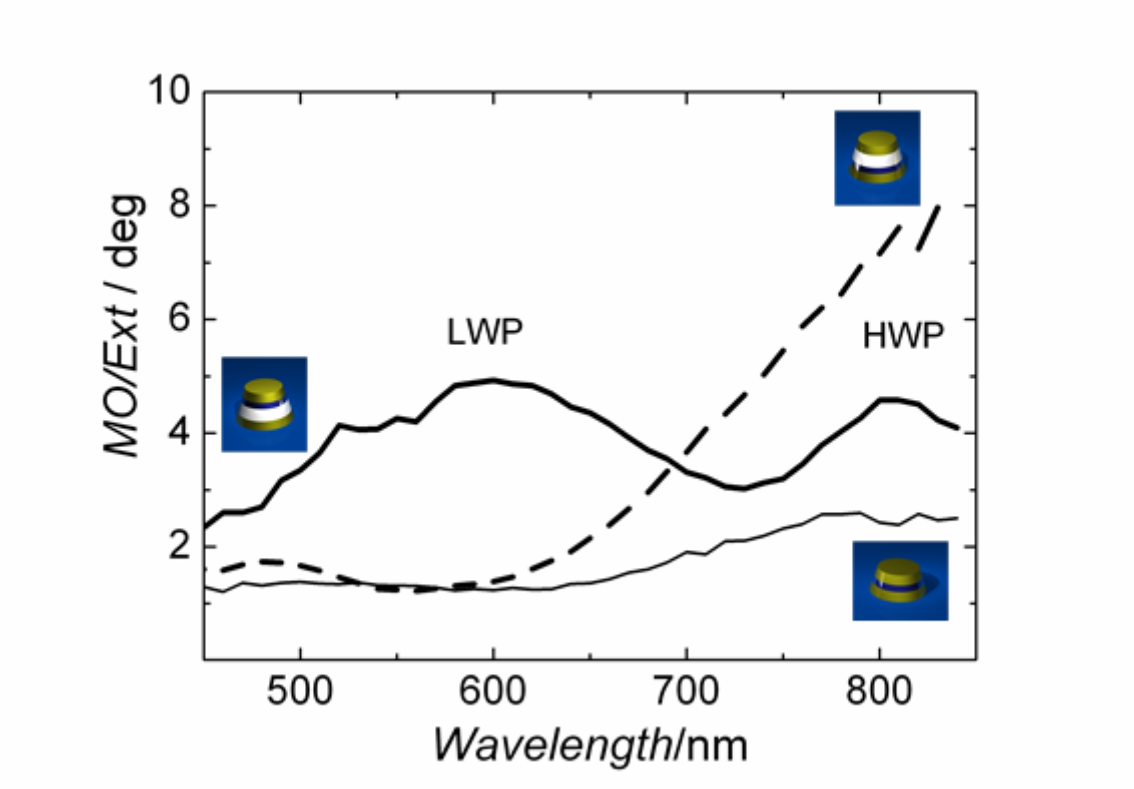

Figure 5. Experimental ratio between the MO activity and the optical extinction, MO/Ext, for the two metal-dielectric (thick solid and dashed lines) and fully metallic (thin solid line) structures.